Am J Cancer Res 2017;7(4):816-830
www.ajcr.us /ISSN:2156-6976/ajcr0048107

Original Article

Molecular mechanism underlying the pharmacological interactions of the protein kinase C-β inhibitor enzastaurin and erlotinib in non-small cell lung cancer cells

Nele Van Der Steen[1,2,3], Lisette Potze[1], Elisa Giovannetti[1], Andrea Cavazzoni[4], Rob Ruijtenbeek[6], Christian Rolfo[2,5], Patrick Pauwels[2,3], Godefridus J Peters[1]

[1]Dept. Medical Oncology, VU University Medical Center, Amsterdam, The Netherlands; [2]Center for Oncological Research, University of Antwerp, Belgium; [3]Department of Pathology, Antwerp University Hospital, Belgium; [4]Department of Clinical and Experimental Medicine, University of Parma, Parma, Italy; [5]Phase I-Early Clinical Trials Unit, Oncology Department, Antwerp University Hospital, Belgium; [6]Pamgene,'s Hertogenbosch, The Netherlands

Received August 12, 2016; Accepted January 12, 2017; Epub April 1, 2017; Published April 15, 2017

Abstract: Erlotinib is commonly used as a second line treatment in non-small cell lung cancer patients with sensitizing EGFR mutations. In EGFR-wild type patients, however the results are limited. Therefore we evaluated whether the combination of the Protein kinase C-β inhibitor enzastaurin with erlotinib could enhance the effect in the A549 and H1650 cell lines. Cytotoxicity of erlotinib, enzastaurin and their 72-h simultaneous combination was assessed with the MTT assay. The pharmacologic interaction was studied using the method of Chou and Talalay, cell cycle perturbations were assessed by flow cytometry and modulation of ERK1/2 and AKT phosphorylation was determined with ELISA. For protein phosphorylation of GSK3β we performed Western Blot analysis and a Pamgene phosphorylation array, while RT-PCR was used to investigate VEGF and VEGFR-2 expression before and after drug treatments. A synergistic interaction was found in both cell lines with mean CI of 0.58 and 0.63 in A549 and H1650 cells, respectively. Enzastaurin alone and in combination with erlotinib increased the percentage of cells in S and G2M phase, mostly in H1650 cells, while AKT, ERK1/2 and GSK3β phosphorylation were reduced in both cell lines. VEGF expression decreased 5.0 and 6.9 fold in A549 cells after enzastaurin alone and with erlotinib, respectively, while in H1650 only enzastaurin caused a relevant reduction in VEGF expression. The array showed differential phosphorylation of EGFR, GSK3β, EphA1 and MK14. In conclusion, enzastaurin is a protein kinase Cβ inhibitor, working on several cellular signaling pathways that are involved in proliferation, apoptosis and angiogenesis. These features make it a good compound for combination therapy. In the present study the combination of enzastaurin and erlotinib gives synergistic results, warranting further investigation.

Keywords: Protein kinase C-beta, epidermal growth factor receptor, erlotinib, enzastaurin, non-small cell lung cancer, GSK-beta, ERK, AKT

Introduction

Non-small cell lung cancer (NSCLC) is currently the leading cause of cancer incidence and mortality worldwide [1]. About 70% of patients are diagnosed with an advanced stage NSCLC. The standard first line treatment for these patients are platinum-doublet based regimens [2], unless molecular profiling shows the presence of actionable mutations/gene rearrangements. In case of EGFR-mutations or ALK rearrangements, EGFR- or ALK- inhibitors have been approved. However, these subgroups are limited to adenocarcinoma histology and comprise about 8% and 3% respectively of this patient population [3, 4].

The EGFR signaling pathway is an important driver pathway which regulates growth, proliferation, differentiation and survival in mammalian cells [5]. The EGF receptor contains an extracellular domain that is involved in ligand binding and receptor dimerization, a hydrophobic domain, involved in interactions between the

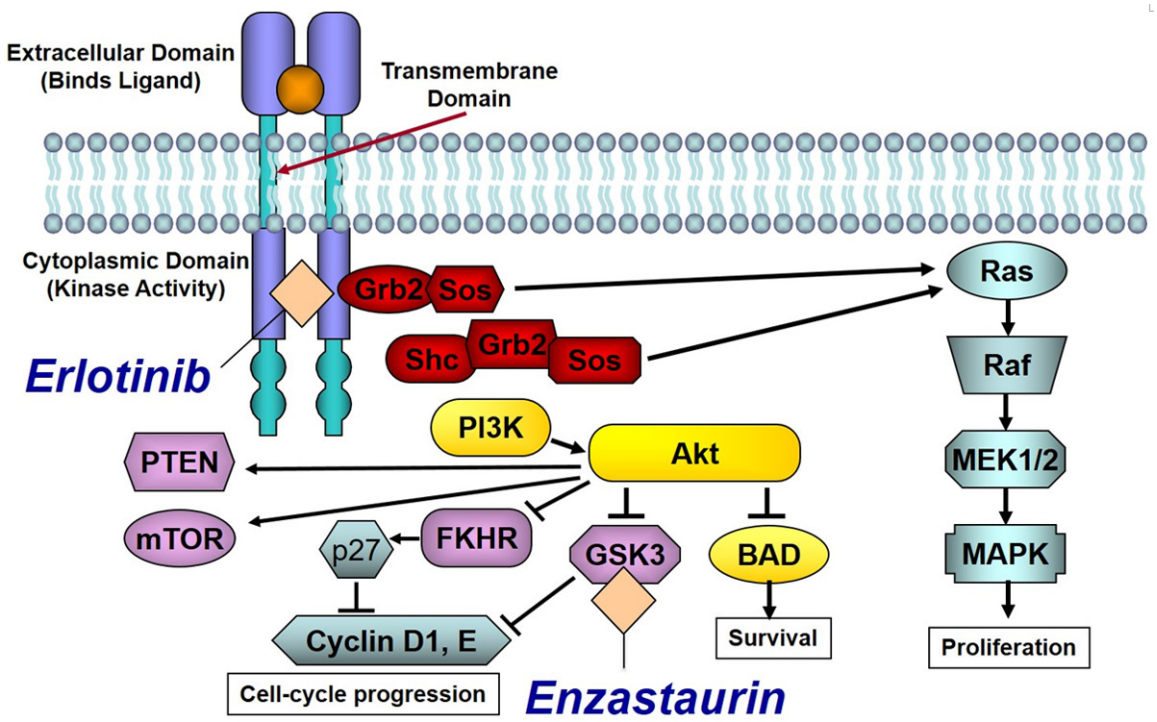

Figure 1. Postulated interaction between enzastaurin and erlotinib in the EGFR pathway. Upon stimulation several downstream pathways such as the PI3K/AKT and RAS pathway are activated. These pathways are involved in the regulation of cell survival, proliferation and apoptosis. The EGFR signaling pathway can be inhibited by erlotinib, which blocks EGFR autophosphorylation, a critical process for the kinase activation, leading to increased apoptosis and decreased cell proliferation.

receptor and the cell membrane, and an intracellular domain with tyrosine kinase enzymatic activity. Stimulation by the ligand EGF or related growth factors leads to receptor homodimerization or hetero-dimerization and thereby activates downstream signaling, involving Ras and Phosphatidyl Inositol 3 Kinase (PI3K) pathways amongst others (**Figure 1**) [5].

Erlotinib is an oral low-molecular weight quinazoline-based agent, which acts as a selective and reversible kinase inhibitor of the epidermal growth factor receptor (EGFR) and is used to treat NSCLC patients with activating EGFR mutations [2], thereby inhibiting downstream signaling. Even though erlotinib is currently used in the treatment of several different cancers, of the minority of patients that present with EGFR-sensitizing mutations, 70-80% is sensitive to this drug. In particular, Ras [6], EGFR T790M mutations [7] and cMET amplification [8] have been associated with primary and acquired resistance to erlotinib.

Enzastaurin is an oral acyclic bisindolylmaleimide, which inhibits Protein Kinase C β2, by ATP competition [9, 10]. The protein kinase C family of enzymes consists of 11 serine/threonine protein kinase isoforms which have a role in signaling cascades of several cellular functions, including cell growth, proliferation and apoptosis as well as cancer growth [11]. In NSCLC, increased phosphorylation and a differential expression of PKC isoforms has been described [12]. These increased levels of PKC have led to overexpression and increased secretion of vascular endothelial growth factor (VEGF) which is involved in neo-angiogenesis [13]. Originally, enzastaurin was evaluated in human tumor xenograft-bearing mice for its anti-angiogenic activity. Due to PKCβ inhibition, a reduction of plasma VEGF levels and a decrease in vessel density in the tumor was shown [14]. However, other molecular mechanisms are also involved in enzastaurin activity, such as the suppression of PI3K/AKT, Glycogen Synthase Kinase 3β (GSK3β) and ribosomal protein S6 [9].

Both erlotinib and enzastaurin can selectively act on aberrant cancer signaling. Because only

the minority of NSCLC-patients presenting with an EGFR activating mutation is sensitive for erlotinib, combining it with enzastaurin could enhance its effect. Therefore, the aim of this study was to investigate whether the combination of erlotinib and enzastaurin could have a synergistic effect in NSCLC cells, and to evaluate the molecular mechanisms underlying the pharmacological interaction. For this purpose we used the NSCLC cells A549 and H1650 cell lines, which are characterized by a Kras mutation and an EGFR activating mutation, resulting in a reduced and increased sensitivity to erlotinib, respectively. The combination with enzastaurin could inhibit the involved pathways, increasing apoptosis and decreasing proliferation.

Material and methods

Drugs and chemicals

Erlotinib (N-(3-ethynylphenyl)-6,7-bis(2-methoxyethoxy0-4-quinazolinamine) was a gift from Roche Pharmaceuticals, while enzastaurin hydrochloride(1H-Pyrrole-2,5-dione,3-(1-methyl-1H-indol-3-yl)-4-[1-[1-(2-pyridinylmethyl)-4-piperidinyl]-1H-indol-3-yl] was a gift from Eli Lilly Corporation. The drugs were dissolved in DMSO and diluted in culture medium before use. RPMI medium, fetal bovine serum (FBS), penicillin (50 IU/ml) and streptomycin (50 µg/ml) were obtained from Gibco (Gaithersburg, MD). All other chemicals were obtained from Sigma (St. Louis, MO).

Cell lines

The human NSCLC cell lines A549 and H1650 were obtained from the American Type Culture Collection (ATCC) (Manassas, VA, USA) and cultured in RPMI (Flow Laboratories Irvine, Scotland) with 10% heat inactivated FBS and 1% penicillin and streptomycin (Gibco Paisley, UK). The cell lines were maintained as monolayer cultures in 75 cm^2 flasks (Costar, Cambridge, MA), at 37°C and 5% CO_2. Cells were harvested with trypsin-EDTA (Invitrogen, Paisley, UK) when they were in exponential growth and the flasks were 75% confluent.

Cytotoxicity assays

Growth inhibition was assayed as described earlier [15]. Shortly, 5000 cells/well were plated in a 96-wells plate and were allowed to adhere for 24 hrs. The cells were treated for 72 hrs with various concentrations (0.1-50 µM or 1-50 µM) of the studied drugs. After treatment, the medium was removed and replaced by 50 µL/well of (3-(4,5-dimethylthiazol-2yl)-2,5 diphenyltetrazolium bromide) MTT solution (final concentration 0.42 mg/ml). The cells were incubated for 3 hours at 37°C. The formed formazan crystals were dissolved in 150 µL/well DMSO, while shaking for 10-20 minutes. The absorbance was measured at 540 nm using a spectrophotometric microplate reader (Tecan Spectrafluor, Salzburg, Austria). The growth inhibition was expressed as the percentage of control (vehicle treated). The 50% inhibitory concentration of cell growth (IC_{50}) was estimated from the growth inhibition curves.

Drug combination studies

To evaluate the possible synergistic effect of both drugs, cells (5000 cells/well) were treated with a constant ratio calculated with respect to drug IC_{50} values. The cytotoxicity of the combination was compared with the cytotoxicity of each drug alone using the combination index (CI) as described by Chou and Talalay [16]. If the CI is lower than 0.8, the drugs work synergistically, 0.8<CI<1.2 means additive, and a CI>1.2 shows an antagonistic effect [17]. The mean CI was calculated from data points of FA>0.5, as values lower are not considered relevant for growth inhibition [18]. The data was processed using the Calcusyn Software (Biosoft, Oxford, UK).

Cell cycle analysis

Flow cytometry was used to determine cell cycle distribution and cell death in the different cell lines treated with erlotinib, enzastaurin, combination or vehicle for 72 hrs. 500,000 cells were plated in a 6-wells plate (Greiner Bio-One GmbH, Frickenhausen, Germany), and treatment started 24 hrs after plating the cells. After 72 hrs floating and adherent cells were collected and transferred into round-bottom FALCON tubes (BD, Franklin Lakes, NJ, USA). After centrifugation the cell pellets were resolved in 1 ml hypotonic propidium iodide (PI) solution (50 mg/ml PI, 0.1% sodium citrate, 0.1% Triton X-100, 0.1 mg/ml ribonuclease A) and stored for 30 minutes on ice. Flow cytometry analyses were performed using FACScan

Table 1. Sensitivity of A549 and H1650 NSCLC cells to erlotinib and enzastaurin and their combination

	IC_{50} (μM)		CI values
Cell line	Erlotinib	Enzastaurin	Fixed ratio
A549	2.88 ± 0.35	8.83 ± 0.05	0.71 ± 0.22
H1650	0.2 ± 0.05	18.83 ± 2.05	0.14 ± 0.17

IC_{50} concentrations of erlotinib and enzastaurin are depicted as means ± SEM (n=3). The combination index (CI) indicates the extent of synergism and was calculated from the average values at fraction affected 0.50 until 0.99 of each separate experiment as shown in **Figure 2**.

(BD Biosciences, Mount View, CA, USA), while data analysis was carried out with CELLQuest™ software, using gates on DNA histograms to estimate the amount of cells in G1, S, and G2/M phases, as well as the apoptotic cells in the sub-G1 region.

ELISA assays

To study the activation of AKT and ERK1/2, 500,000 cells were exposed to IC_{50} values of enzastaurin, erlotinib and enzastaurin-erlotinib combination for 72 hrs. Proteins were isolated and ELISA assays (Biosource International, Camarillo, CA, USA) for total AKT, phospho-AKT at serine residue 473 (AKT[pS473]), total ERK1/2 and dual-phosphorylated ERK1 at threonine 202 and tyrosine 204 (ERK1[pTpY-202/204]) and dual-phosphorylated ERK2 at threonine 185 and tyrosine 187 (ERK2[pTpY-185/187]) were used for the analysis of the activation of AKT and ERK1/2, respectively. Analysis was performed according to the manufacturer's protocol. All results were normalized for protein content and the ratios of phosphorylation/total were calculated [19].

VEGF levels in the medium were determined with the R&D VEGF ELISA (R&D diagnostics, Minneapolis, USA), according to the manufacturers protocol. Of each sample, 200 μl of medium was taken, centrifuged for 20 min at 1000 g. A calibration line was included in each plate.

Real-time qRT-PCR

To study differential gene expression, cells were treated with enzastaurin, erlotinib and enzastaurin-erlotinib combination for 72 hrs. RNA extraction was performed using TRI REAGENT LS (Sigma-Aldrich, Zwijndrecht, the Netherlands) and reverse transcribed using the DyNAMO cDNA synthesis kit for qRT-PCR (Thermo Fisher Scientific, Landsmeer, the Netherlands).

Primers and probes for VEGF and VEGFR-2 (Hs00173626_m1 and Hs00176676_m1, respectively) and for EGFR were obtained from Applied Biosystems. Data were normalized to β-actin and target gene quantitation was performed using standard curves obtained with dilutions of cDNA from Quantitative-PCR Human Reference Total-RNA (Stratagene, La Jolla, CA, USA) [19].

Western blot

To evaluate the effect of the drugs on protein concentration we performed Western Blot analysis. Cells were treated for 72 hrs with vehicle or IC_{50} values of enzastaurin and erlotinib (single or simultaneous combination). Cells were harvested and redisolved in lysis buffer (0.1% (v/v) Triton X-100, 10% glycerol, 150 mM NaCl, 10 mM Tris-HCL pH 7.6, 50 mM β-glycerophosphate, and 5 mM EDTA) and protein concentration was determined by the Biorad assay. Samples were denatured in sample buffer containing SDS and β-mercaptoethanol and equal amounts of protein were loaded and separated on 8-15% SDS-PAGE gels and transferred to Odyssey polyvinylidene fluoride membranes [20]. Next, the membranes were blocked with 5% nonfat dry milk/TBST and incubated overnight at 4°C with the primary antibodies diluted in 5% BSA/TBST. After washing, the membranes were incubated with secondary antibody (1:1 Li-Cor: PBS) in the dark for 1 hr and washed again. Detection was performed on the Odyssey machine using Li-Cor.

The following primary antibodies were used: GSK3β *1:1000*, phospho-GSK3β (Ser9) *1:1000* (from Cell Signaling Technology); Cdc25C *1:1000*, phospho-Cdc25C (Ser 216) *1:1000,* CDK2 *1:500*, phospo-CDK2 (Thr160) *1:500*, CHK2 *1:1000*, and, as a loading control, β-actin *1:10000* (Sigma Aldrich). The fluorescent secondary antibodies were goat anti-rabbit-IRDye800Cw (Westburg 926-32210D) and goat anti-mouse-IRDye680 (Westburg 926-32220D) *1:10000*.

PAMgene array

A PAMchip array was used to analyse the effect of the drugs on tyrosine kinase activity

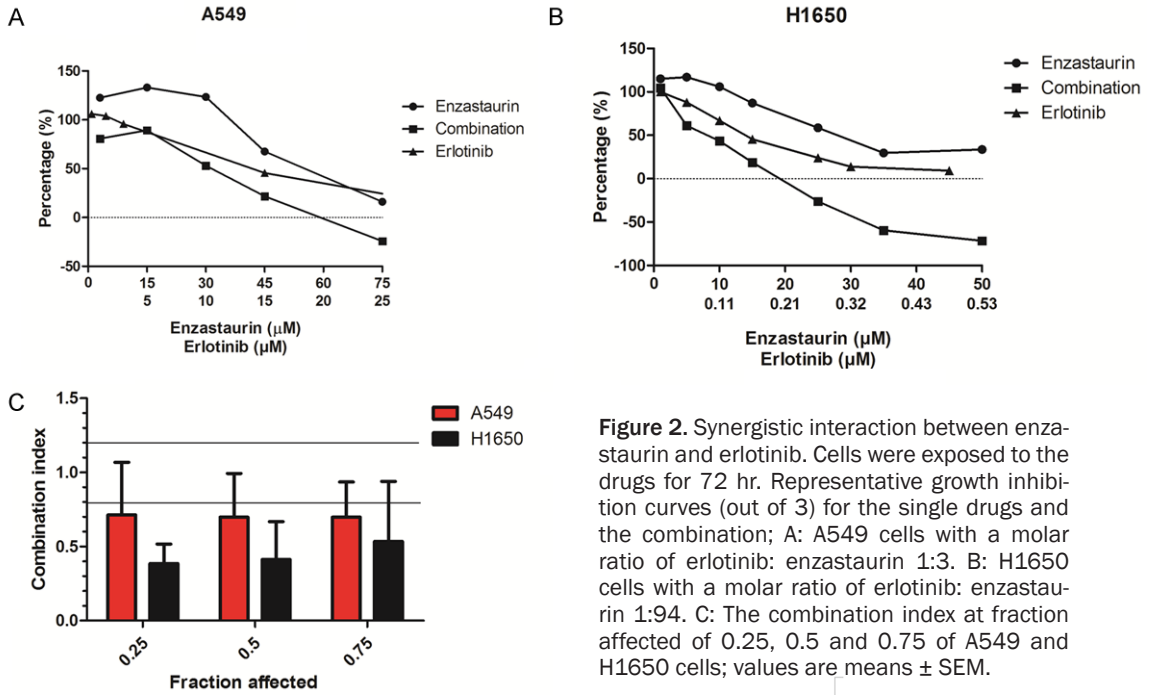

Figure 2. Synergistic interaction between enzastaurin and erlotinib. Cells were exposed to the drugs for 72 hr. Representative growth inhibition curves (out of 3) for the single drugs and the combination; A: A549 cells with a molar ratio of erlotinib: enzastaurin 1:3. B: H1650 cells with a molar ratio of erlotinib: enzastaurin 1:94. C: The combination index at fraction affected of 0.25, 0.5 and 0.75 of A549 and H1650 cells; values are means ± SEM.

(PAMgene,'s Hertogenbosch, the Netherlands). The Pamchip contains 136 phosphorylation sites of 144 peptides each consisting of 15 amino-acids. The 13 amino-carboxylic acids (R-COOH) of each peptide correspond to known or putative phosphorylation sites of tyrosine kinases. Experiments were performed and analyzed as described previously [21]. Briefly, A549 (10^7 cells/ml) cells were stimulated with epidermal growth factor (50 μg/ml) for 5 min and subsequently exposed for 2 hours to 4.6 μM erlotinib, 10 μM enzastaurin or their combination. Cells were harvested, snap-frozen and stored at -80°C until analysis. Cell pellets were lysed during 20 min at 4°C with Mammalian Protein Extraction Reagent (M-PER), phosphatase and protease inhibitors (Thermo Scientific, Rockford, IL, USA). Next, the lysates were centrifuged (15 min at 10000g). 40 μl of sample mix was subsequently prepared using reaction buffer 1× ABL buffer (Westburg), 100 μM ATP (Sigma-Aldrich), fluorescent labeled antibody PY20 (Exalpha, Maynard, MA), 5 μg of (lysate) protein and DMSO. The arrays were blocked using 2% BSA and the sample mix was loaded. After incubation at 30°C, analysis was started for 60 cycles using a Pamstation 96 instrument (Pamgene International). Repeated fluorescent imaging took place throughout the analysis with a 12-bit charge-coupled device (CCD) camera, thus real-time monitoring fluorescence. Spot intensity was corrected for local background and initial phosphorylation rates (V_{ini}) were calculated using Bionavigator software 5.1 (Pamgene International).

Results

Growth inhibition and pharmacological interaction studies

Previous experiments showed a dose dependent inhibition of cell growth with erlotinib in A549 and H1650 cells [19]. For the A549 cells a dose dependent inhibition of cell growth was also observed after enzastaurin treatment in A549 cells with a mean IC_{50} ± SEM value of 8.83 ± 0.05 SEM [10] (**Table 1**). A dose dependent inhibition of cell growth was observed in H1650 cells treated with enzastaurin, with a mean IC_{50} ± SEM of 18.83 ± 2.05 μM (**Figure 2**). When treating both cell lines with a constant ratio of both drugs simultaneously, a synergistic effect was obtained in both the A549 and H1650 cell lines, with a mean ± SEM CI of 0.58 ± 0.24 and 0.63 ± 0.03, respectively (**Table 1**).

Cell cycle modulation and induction of apoptosis

Flow cytometry with PI was performed to evaluate the effect on the cell cycle distribution and

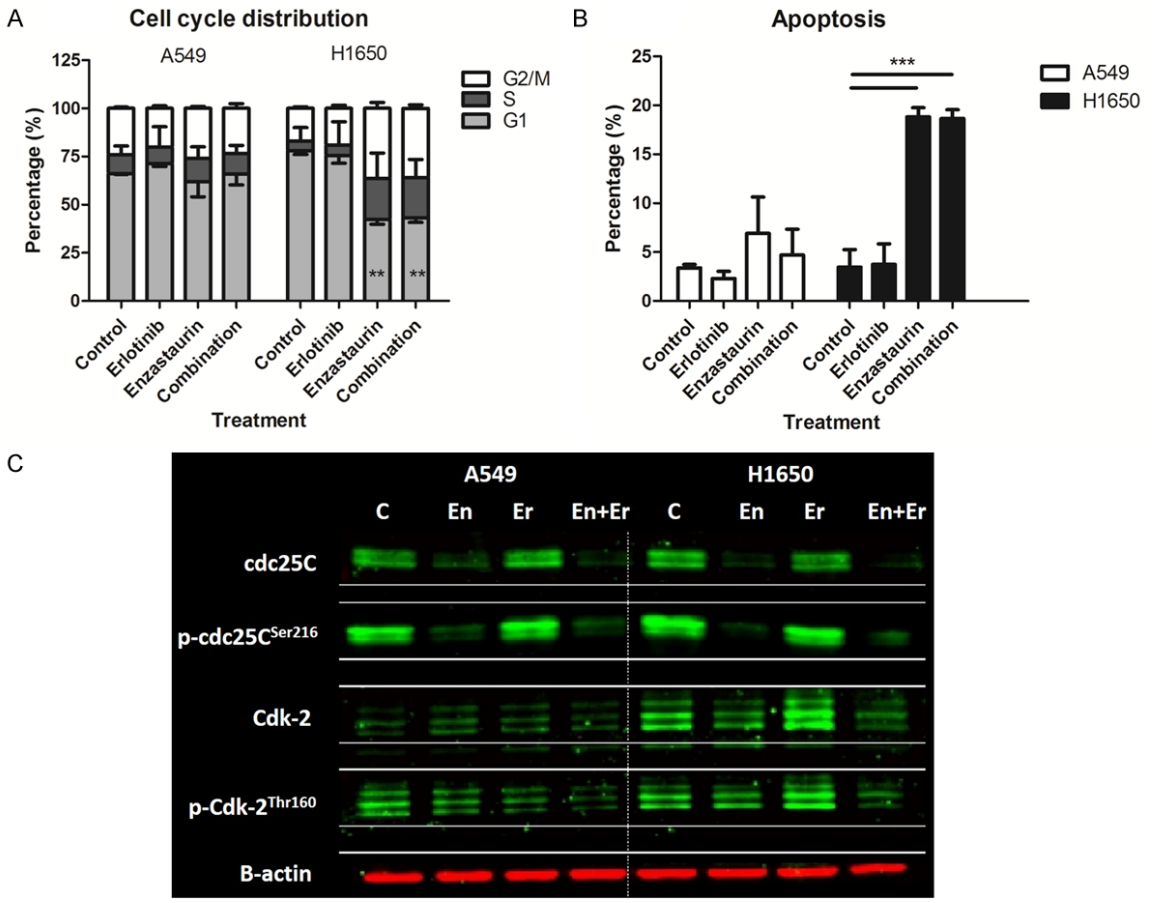

Figure 3. Effect of erlotinib (Er) and enzastaurin (En) on cell cycle distribution and cell cycle proteins. Cells were treated for 72 h at their IC_{50} values or with 0.1% DMSO, A549: 2.88 μM Er and 8.83 μM En; H1650: 0.2 μM Er and 18.83 μM En. Values are means ± SEM. **: P<0.01; ***: P<0.001 as compared to control (A) Cell cycle distribution. (B) Percentage of cells in sub-G1 phase. (C) Western Blotting of phosphorylated cell cycle proteins cdc-25C and CDK2.

to determine the extent of cell kill (**Figure 3**). In A549 cells erlotinib increased the G1 phase from 66.2% to 71.3%, while enzastaurin and the combination increased the S-phase from 9.8% to 11.9% and 10.8%, respectively. In H1650 cells the treatment with enzastaurin and the combination significantly increased the S phase from 4.9% to 21.3% and 21.0%, respectively, as well as the G2M phase from 17.0% to 36.4% and 35.9%. In contrast, the G1 phase decreased from 78.0% to 42.3% and 43.1%. Erlotinib alone did not cause cell cycle arrest in H1650 cells. In A549 cells only a low increase in cell death was observed after treatment with enzastaurin or the combination from 3.4% to 6.9% and 4.7%, respectively. In H1650, however, enzastaurin and the combination induced a marked cell kill from 3.5% to 18.8% and 18.7%, respectively (**Figure 3**). In order to determine how the alteration in the cell cycle distribution was regulated we measured several cell cycle specific proteins. First, both expression and phosphorylation of cdc25c, a key regulator of the G2/M checkpoint, were determined. Enzastaurin alone was sufficient to downregulate both expression and phosphorylation of cdc25c, the same effect could be observed after combination treatment. CDK2 plays a role during the G1- and S-phases of the cell cycle. CDK2 had an overall lower expression in A549 cells as compared to H1650 cells, but in both cell lines enzastaurin caused a decrease in phosphorylation, which was even enhanced after combined treatment with erlotinib (**Figure 3**).

Modulation of AKT, ERK1/2 and GSK3β phosphorylation

EGFR signaling is mainly transduced trough the AKT and ERK1/2 pathway. To investigate whether combining erlotinib with enzastaurin

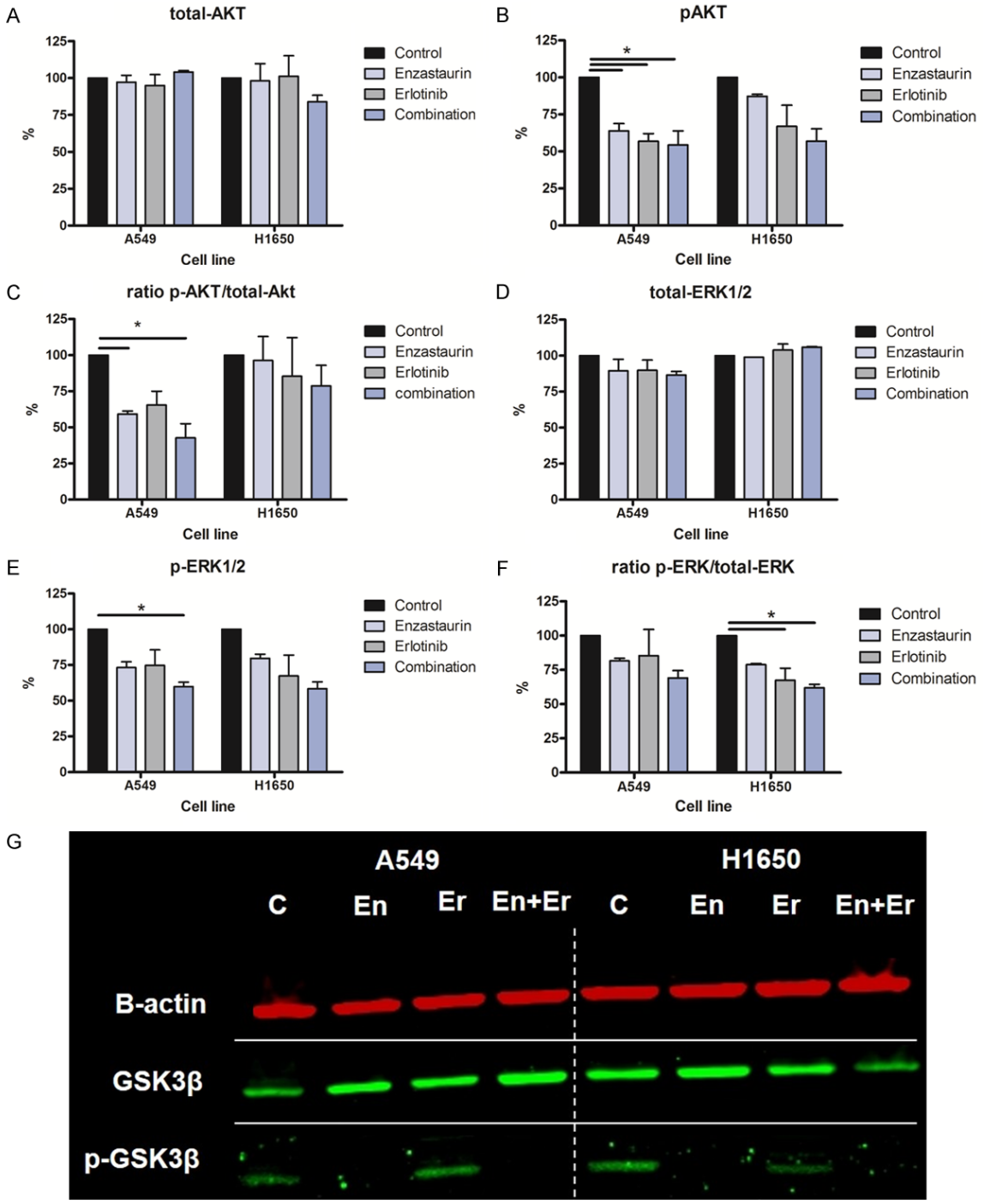

Figure 4. Inhibition of phosphorylation by enzastaurin, erlotinib and their combination as measured by ELISA (A-F) or Western Blot. Cells were treated during 72h at their IC_{50} values as specified in **Figure 3**. *: P<0.05, **: P<0.01. Modulation of total AKT (A), p-AKT (B), ratio of p-AKT/AKT (C), modulation of total ERK1/2 (D), p-ERK1/2 (E), ratio of p-ERK1/2 and ERK (F), and GSK3 β (G). Means ± SEM obtained from two independent experiments in triplicate (A-F) or representative blot out of 3 separate experiments (G).

decreases this signaling, we evaluated the phosphorylation of these proteins. Whereas the total expression of both proteins stayed stable after the different treatments, we found a decreased ratio of p-AKT/total AKT in A549 cells. Enzastaurin or erlotinib in monotherapy decreased this ratio by 40%, while the combination of these drugs even showed a 60%

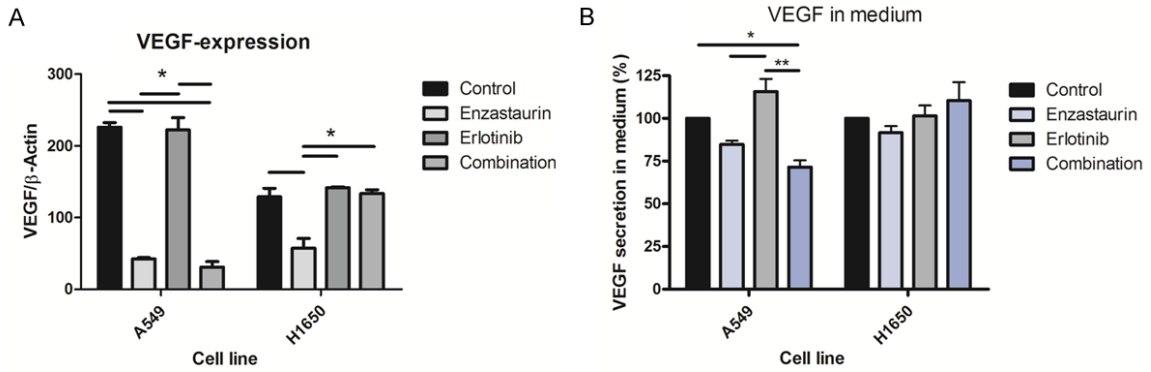

Figure 5. Modulation of VEGF mRNA expression (A) and VEGF-secretion (B). Measured by RT-PCR and ELISA respectively, mean values (± SEM) obtained from two independent experiments in triplicates. Cells were treated during 72 h at their IC_{50} values as specified in **Figure 3**. *: P<0.05, **: P<0.01.

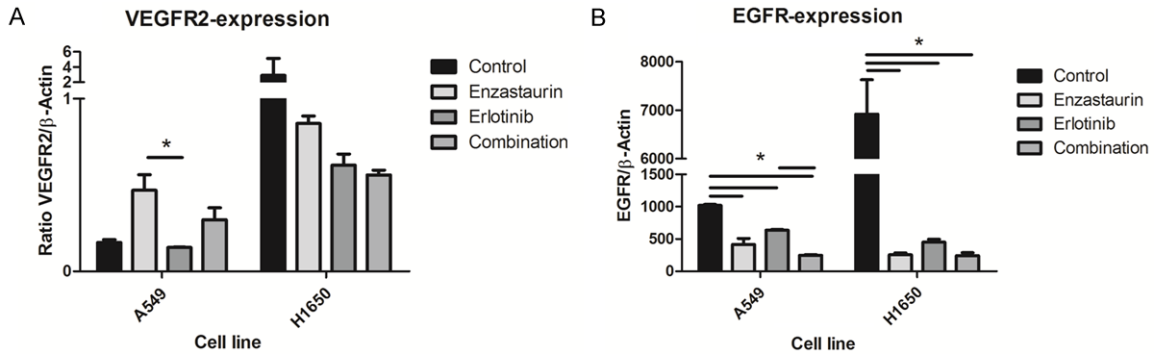

Figure 6. VEGFR-2 (A) and EGFR (B) mRNA expression as determined by real time RT-PCR after 72 hr treatment at IC_{50} values of the drugs as specified in **Figure 3**. Mean values ± SEM obtained from two independent experiments in triplicates. *: P<0.05, **: P<0.01.

reduction. In contrast, only a modulation of 20% in p-AKT/total AKT was observed in H1650 cells after combined treatment (**Figure 4C**).

Regarding the ratio of phospho-ERK/total ERK, a decrease of 20% after enzastaurin monotherapy was observed in H1650 cells, while erlotinib reduced this ratio with 30% and the combination of both drugs by 40%. Similarly, in A549 cells a reduction of 20, 15 and 30% was observed after enzastaurin, erlotinib and combination treatment respectively (**Figure 4F**).

Since enzastaurin affects several cellular signaling pathways, we also focused on GSK3β phosphorylation, which was studied by western blot analysis. These results showed that the phosphorylation of GSK3β is already strongly inhibited in both cell lines by treatment with enzastaurin alone. Similarly, the simultaneous combination of both drugs reduced GSK3β phosphorylation to undetectable levels (**Figure 4G**).

Modulation of VEGF and VEGFR-2 mRNA expression

Since enzastaurin is known for its anti-angiogenic effect and the PKC pathway is involved in angiogenesis we performed qRT-PCR to evaluate the modulation of the expression of VEGF and VEGFR-2.

A549 cells treated with enzastaurin or the combination of enzastaurin and erlotinib showed a 5.0 and 6.9 fold decrease in VEGF expression, respectively. On the other hand, erlotinib alone did not show a relevant decrease in VEGF expression. A 2.4 fold decrease was observed in H1650 cells treated with enzastaurin, while treatment with erlotinib and the combination of both drugs did not alter VEGF expression in H1650 cells (**Figure 5A**). Despite the strong decrease in VEGF expression, secretion of VEGF was hardly affected by the drugs; only in A549 cells enzastaurin reduced VEGF secretion by 15%, while the combination decreased

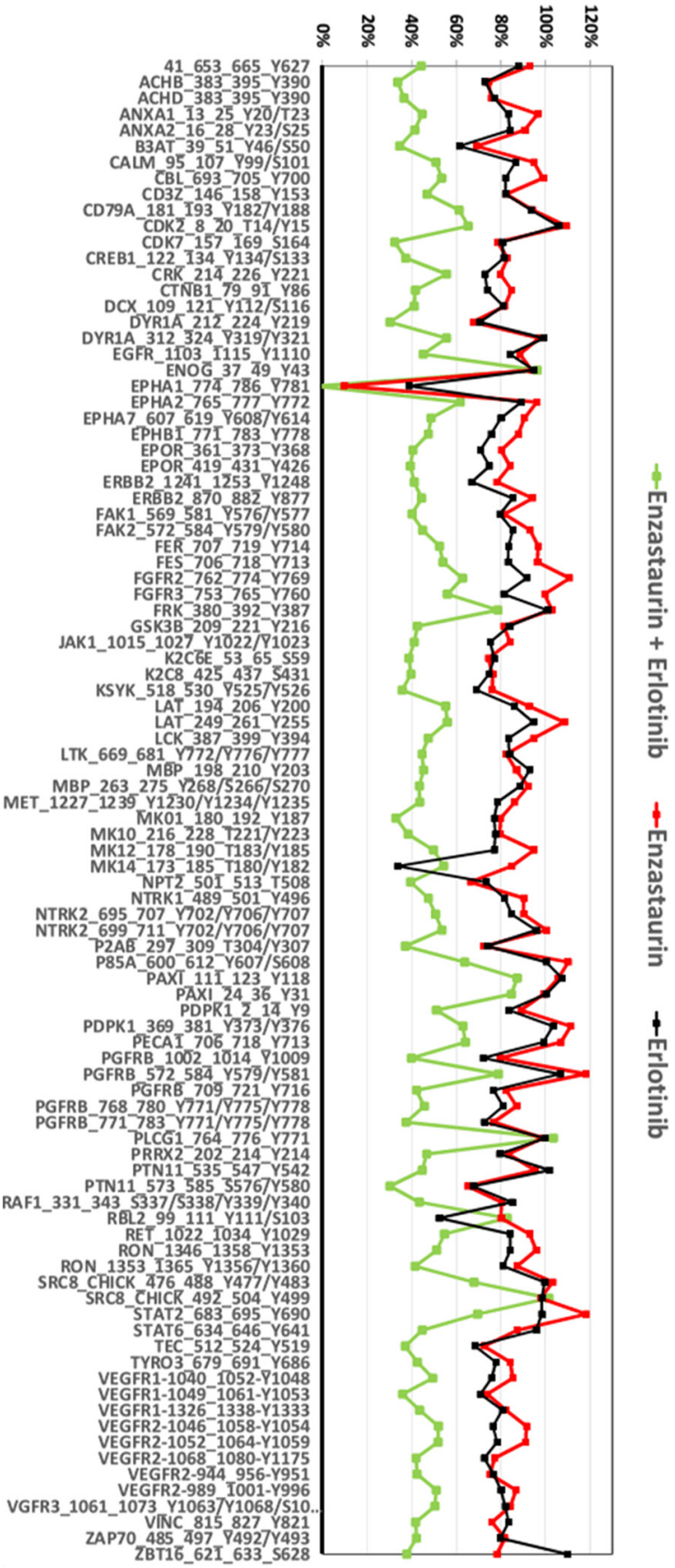

Figure 7. Effect of enzastaurin, erlotinib and their combination on phosphorylation sites. A549 cells were exposed for 2 hrs (after a challenge with EGF) to 4.6 μM erlotinib, 10 μM enzastaurin and their combination. Subsequently phosphorylation activity was determined in lysates of these cells. The figure shows the initial velocity (V-ini) of phosphorylation of those peptides where a reliable signal was found. Values in the absence of drugs (0.1% DMSO) were set at 100%.

secretion by 30%. Erlotinib treatment alone caused no changes in VEGF secretion (**Figure 5A**).

The expression of VEGFR-2 in A549 cells increased 1.7 and 3.0 fold after treatment with the combination or enzastaurin, respectively, whereas erlotinib did not alter its expression. In H1650 cells VEGFR-2 expression dropped after treatment with enzastaurin, erlotinib and the combination in comparison to the control (**Figure 6A**). There was no significant difference in VEGFR-2 expression between cells treated with erlotinib, enzastaurin or their combination.

The EGFR levels of the control in H1650 cells are 7-fold higher when compared to the A549. Nevertheless, in both cell lines erlotinib, enzastaurin and the combination all decreased EGFR expression, with a much more pronounced decrease in the H1650 cells. The lowest levels of EGFR were obtained after treatment with the combination of both drugs (**Figure 6B**).

Modulation of protein tyrosine kinase activity by enzastaurin and erlotinib

The Pamgene array consists of 144 peptides representing known and assumed phos-

phorylation sites. With this assay, the activity and inhibition of the tyrosine kinases in exposed cells can be determined in real-time (**Figure 7**). From these peptides, signal intensity of 50 sites was considered to be too low to evaluate. Enzastaurin or erlotinib monotherapy led to a reduction of 11 and 15% in EGFR phosphorylation speed, respectively, whereas the combination led to a 55% reduction. On the remaining peptides, erlotinib caused an overall decrease in tyrosine kinase activity of 20%. A strong decrease in MK14 (MAPK14) and RBL2 (retinoblastoma-like 2) phosphorylation was observed, whereas these effects were abrogated after combining erlotinib with enzastaurin. Erlotinib monotherapy only caused a 20% decrease of EGFR phosphorylation. Enzastaurin treatment resulted in an overall reduction of phosphorylation speed of 20%, whereas combination of erlotinib and enzastaurin, led to an overall decrease of 60%, with a total abrogation of EPHA1 phosphorylation. Furthermore, the enzastaurin induced decrease in phosphorylation of MK14 and RBL2 was abrogated after combination therapy. In contrast, the phosphorylation of SRC8 (CTTN, Cortactin) and PLCG1 was increased in comparison with that of other peptides, whereas this was not the case after treatment with erlotinib or enzastaurin alone.

Discussion

In the present study, we demonstrated a synergistic interaction of the PKCβ inhibitor enzastaurin and the EGFR inhibitor erlotinib in A549 and H1650 NSCLC cell lines. It has been shown that sensitizing mutations in EGFR are good biomarkers for erlotinib efficiency [4]. For enzastaurin, no clear biomarkers have been found, although evidence suggests that proteins related with the JAK/STAT pathway might serve as predictors for activity [22]. Here we investigated whether the combination of these two drugs is synergistic in a cell line with sensitizing EGFR mutations (H1650), as well as a cell line without EGFR mutations (A549).

Several studies have shown the importance of modulating the cell cycle in the effect of drug combinations [23]. Drugs acting at different stages of the cell cycle might potentiate each other's effect. Previous studies showed that PKC can mediate cell cycle transitions [24]. In the A549 cells the effects on cell cycle arrest were minimal, but in the H1650 an increased portion of the cells were in the S- or G2/M-phase after treatment with enzastaurin alone or in combination. Erlotinib by itself did not result in cell cycle arrest in both cells.

CDK2 plays an active role in the transition between the S- and G2-phase, controlled by phosphorylation at Thr160 [25]. Western Blotting revealed that phosphorylation at the CDK2-Thr160 site was strongly decreased after the combination therapy and to a lesser extent after enzastaurin treatment. This decrease might cause the S-phase arrest.

Cdc25C is inactive when phosphorylated at its Ser216 residue and plays a role in the G2/M transition of the cell cycle [26]. It has been shown that cdc25C promotes the M-phase transition by phosphorylating and activating cdc2 [27]. Previous studies have shown that PKC induces the phosphorylation of cdc25C, thus promoting the G2 to M transition. When inhibiting PKC with either antibodies or antisense DNA, a G2/M phase arrest has been demonstrated [28]. Our results indeed show a strong decrease in both total cdc25C levels, and in cdc25C-Ser216 phosphorylation, after treatment with either enzastaurin or in the combination, thus explaining the G2/M-phase arrest.

In the present study, no induction of apoptosis was observed, in contrast to studies combining either erlotinib or enzastaurin with pemetrexed [10, 19]. Since both erlotinib and enzastaurin are not known as cytotoxic and cytostatic drugs, this might explain the lack of apoptosis induction as compared to the combinations with the antimetabolite pemetrexed. Hence combination of enzastaurin and erlotinib can increase arrest in several cell cycle checkpoints, without inducing apoptosis.

Regarding the downstream effectors of PKCβ- and EGFR-signaling, a decrease in the phosphorylation of AKT, ERK1 and GSK3β was observed. Since AKT is a downstream effector of both PKCβ and EGFR [29, 30], levels of phospho-AKT were decreased after all treatments in both cell lines. In A549 cells the decrease of phospho-AKT/total AKT ratio was most pronounced. The other downstream target of both PKCβ and EGFR signaling [31, 32], ERK1/2 showed a decrease in phosphorylation at all

treatment conditions. Moreover, the ratio phospho-ERK1/2 over total ERK1/2 was decreased in both cell lines after drug treatment. Since GSK3β is an effector of PKCβ [33] but not of EGFR, a decrease in phosphorylation was only observed after treatment with enzastaurin or the combination, reported earlier for enzastaurin in different cell lines [9, 10, 34, 35] inducing a decrease in p-AKT for 24 h [10]. These results suggest that they may be used as pharmacodynamic markers of enzastaurin activity.

Although enzastaurin has a direct effect on several human cancer cells [10], it was originally developed as anti-angiogenic compound. Enzastaurin decreased intratumoral vessel density and VEGF expression in several human xenografts and NSCLC cell lines [10, 14], and A549 cells in the present study. However, the drug combination had no effect on VEGF expression in H1650 cells, suggesting that several mechanisms might be involved in VEGF expression regulation. Although *in vitro* experiments showed a reduction of VEGF in the medium [10], in a clinical study enzastaurin increased VEGF plasma levels which were further increased by the combination of enzastaurin-pemetrexed [36, 37]. However, another clinical trial in advanced NSCLC patients treated with enzastaurin did not show a consistent change in VEGF plasma levels, but could associate low baseline VEGF levels with longer progression free survival [36]. Further research is warranted to clarify these results.

Finally, we also studied the VEGFR-2 expression, which was increased after treatment with enzastaurin in both cell lines. This might be explained by the reduction of VEGF expression, inducing a feedback mechanism on VEGFR-2 expression in the cells. In case of a highly activated VEGFR-2 it would be useful to use a combination with a drug active against VEGFR-2 (i.e sorafenib). Therefore, these data showed promising results, which need further investigation, possibly also in combination with other targeted compounds.

When comparing the kinase activity data of the Pamgene analysis, several trends can be seen. Phosphorylation of EGFR at Tyr1110 is linked to its activation [38]. Tyr1110 phosphorylation is affected by erlotinib treatment, and has been correlated with EGFR mutations [38].

GSK3β is a downstream target of both enzastaurin [9] and erlotinib [39] through AKT. Active GSK3β induces degradation of cyclin-D1, thus inhibiting cell cycle G1 transition. In turn, GSK3β is inhibited by AKT under normal conditions through phosphorylation at the regulatory Ser9 position. A reduction in phosphorylation speed was also observed at the active site Tyr216 residue both after enzastaurin (19%) and erlotinib treatment (16%). The combination of both inhibitors even led to a 57% reduction of phosphorylation. GSK3β plays a role in the Wnt-pathway were it phosphorylates β-catenin, thus targeting it for degradation [40]. By phosphorylating β-catenin, this downstream target of Wnt will not translocate to the nucleus to exert its activator transcription function [41]. When GSK3β is phosphorylated at Tyr216, it is ubiquitinated by β-TrCP and marked for degradation, thus promoting β-catenin stability and Wnt-signaling. So, when Tyr216-phosphorylation of GSK3β is reduced, this might also lower signaling through the oncogenic Wnt-pathway [40].

EphA1 (Ephrin Receptor A1) is a member of the Eph superfamily. These receptors mainly play roles in cell-cell interactions and migration, with ligand and receptor sitting on the opposite cell membranes of contacting cells. Several Ephrin A ligands can activate bidirectional signaling, with forward signaling downstream of the receptor and reversed signaling downstream of the ligand [42]. These receptors and ligands have been associated with both tumor growth and suppression [43-47]. Which factors influence the outcome has not yet been elucidated. Moreover, several processes seem to be independent of kinase activity of the receptors [48]. We saw a strong downregulation of phosphorylation at the Y781 site of the EphA1 receptor after treatment with enzastaurin or erlotinib and even a total abrogation of phosphorylation after treatment with the combination. A possible explanation is that a downregulation of integrin adhesion is caused in a kinase-dependent manner [49].

MK14 encodes for p38 MAPK [50]. This protein is activated when it is dually phosphorylated at Thr180 Tyr182 and is located at a crossroad of several signaling pathways e.g. JNK and Rho. Activation of p38 MAPK strongly declines after erlotinib treatment, with the effect being lower after enzastaurin or combination treatment. p38 MAPK is a downstream target of PKCβ. In

hepatocellular carcinoma, p38 MAPK phosphorylation has been correlated with metastatic potential of the cells. Enzastaurin inhibits PKCβ-activation and decreases p38 MAPK phosphorylation, thus affecting the invasive and migratory potential of the cells [51]. Phosphorylated p38 MAPK has also been shown to play a role in the EGFR signaling pathway. In particular it degrades MDM2, thus preventing p53 degradation. Next p53 translocates to the nucleus and regulates the transcription of EGFR [52]. When erlotinib blocks EGFR signaling, the phosphorylation speed of p38 MAPK strongly decreases. It has been shown that EGFR-TKIs suppress the internalization of EGFR [53]. This might result in a feedback to p38 MAPK, decreasing its phosphorylation and activity.

Our extensive *in vitro* studies are essential for the judicious selection of the best combination and models to be tested in future *in vivo* tumor models, as well as to evaluate the role of potential biomarkers which can predict drug activity. Earlier *in vivo* studies in the development of enzastaurin showed effects on angiogenesis, such as VEGF levels [9, 54], which were also found in clinical studies [37]. Furthermore, in both cultured tumor cells and in xenograft tumor tissues from the same cell lines, enzastaurin inhibited the phosphorylation pGSK3β [9, 54], and a more potent inhibition on protein expression was observed when it was combined with another EGFR-TKI, gefitinib [54]. Several other *in vivo* studies showed that both enzastaurin and erlotinib affected the Akt pathway [9, 10, 19]. Therefore, future *in vivo* studies on the combination of erlotinib and enzastaurin should investigate both the overall antitumor effect, and whether the mechanism will include effects on signaling and angiogenesis.

In conclusion enzastaurin is a PKCβ inhibitor, acting on several cellular signaling pathways that are involved in proliferation, apoptosis and angiogenesis. These features make it a good compound to combine with other compounds in combination therapy. Although it is no longer in clinical development for NSCLC, research into enzastaurin and related compounds is still ongoing in other cancer types (eg glioblastoma [55] and colorectal cancer [56]) and non-cancer related illnesses (cardiovascular conditions, diabetes, bipolar disorder and transplantation) [57].

Acknowledgements

NVS is funded by the Institute for Innovation, Science and Technology Flanders (IWT): grant number 121114. Funded by grants from Cancer Center Amsterdam (CCA) Foundation (to EG and GJP), Associazione Italiana per la Ricerca sul Cancro (AIRC), and Regione Toscana Bando FAS Salute (to EG). This study was also supported by Eli Lilly & Co, Houten, the Netherlands (to GJP).

Disclosure of conflict of interest

None.

Address correspondence to: Godefridus J Peters, Department of Medical Oncology, VU University Medical Center, De Boelelaan 1117, 1081 HV, Amsterdam, The Netherlands. Tel: +31-20-4442633; Fax: +31-20-4443844; E-mail: gj.peters@vumc.nl

References

[1] American Cancer Society, Cancer facts & figures 2016. 2016.

[2] Besse B, Adjei A, Baas P, Meldgaard P, Nicolson M, Paz-Ares L, Reck M, Smit EF, Syrigos K, Stahel R, Felip E, Peters S; Panel Members; ESMO. 2nd ESMO Consensus Conference on Lung Cancer: non-small-cell lung cancer first-line/second and further lines in advanced disease. Ann Oncol 2014; 25: 1475-1484.

[3] Soda M, Choi YL, Enomoto M, Takada S, Yamashita Y, Ishikawa S, Fujiwara S, Watanabe H, Kurashina K, Hatanaka H, Bando M, Ohno S, Ishikawa Y, Aburatani H, Niki T, Sohara Y, Sugiyama Y, Mano H. Identification of the transforming EML4-ALK fusion gene in non-small-cell lung cancer. Nature 2007; 448: 561-566.

[4] Lynch TJ, Bell DW, Sordella R, Gurubhagavatula S, Okimoto RA, Brannigan BW, Harris PL, Haserlat SM, Supko JG, Haluska FG, Louis DN, Christiani DC, Settleman J, Haber DA. Activating mutations in the epidermal growth factor receptor underlying responsiveness of non-small-cell lung cancer to gefitinib. N Engl J Med 2004; 350: 2129-39.

[5] Carcereny E, Morán T, Capdevila L, Cros S, Vilà L, de Los Llanos Gil M, Remón J, Rosell R. The epidermal growth factor receptor (EGFR) in lung cancer. Transl Respir Med 2015; 3: 1.

[6] Linardou H, Dahabreh IJ, Kanaloupiti D, Siannis F, Bafaloukos D, Kosmidis P, Papadimitriou CA, Murray S. Assessment of somatic k-RAS mutations as a mechanism associated

with resistance to EGFR-targeted agents: a systematic review and meta-analysis of studies in advanced non-small-cell lung cancer and metastatic colorectal cancer. Lancet Oncol 2008; 9: 962-972.

[7] Kobayashi K and Hagiwara K. Epidermal growth factor receptor (EGFR) mutation and personalized therapy in advanced nonsmall cell lung cancer (NSCLC). Target Oncol 2013; 8: 27-33.

[8] Engelman JA, Zejnullahu K, Mitsudomi T, Song Y, Hyland C, Park JO, Lindeman N, Gale CM, Zhao X, Christensen J, Kosaka T, Holmes AJ, Rogers AM, Cappuzzo F, Mok T, Lee C, Johnson BE, Cantley LC, Jänne PA. MET amplification leads to gefitinib resistance in lung cancer by activating ERBB3 signaling. Science 2007; 316: 1039-1043.

[9] Graff JR, McNulty AM, Hanna KR, Konicek BW, Lynch RL, Bailey SN, Banks C, Capen A, Goode R, Lewis JE, Sams L, Huss KL, Campbell RM, Iversen PW, Neubauer BL, Brown TJ, Musib L, Geeganage S, Thornton D. The protein kinase Cβ-selective inhibitor, Enzastaurin (LY317615. HCl), suppresses signaling through the AKT pathway, induces apoptosis, and suppresses growth of human colon cancer and glioblastoma xenografts. Cancer Res 2005; 65: 7462-7469.

[10] Tekle C, Giovannetti E, Sigmond J, Graff JR, Smid K, Peters GJ. Molecular pathways involved in the synergistic interaction of the PKCβ inhibitor enzastaurin with the antifolate pemetrexed in non-small cell lung cancer cells. Br J Cancer 2008; 99: 750-759.

[11] Garg R, Benedetti LG, Abera MB, Wang H, Abba M, Kazanietz MG. Protein kinase C and cancer: what we know and what we do not. Oncogene 2014; 33: 5225-37.

[12] Clark AS, West KA, Blumberg PM, Dennis PA. Altered protein kinase C (PKC) isoforms in non-small cell lung cancer cells: PKCdelta promotes cellular survival and chemotherapeutic resistance. Cancer Res 2003; 63: 780-786.

[13] Hofmann J. Protein kinase C isozymes as potential targets for anticancer therapy. Curr Cancer Drug Target 2004; 4: 125-46.

[14] Keyes KA, Mann L, Sherman M, Galbreath E, Schirtzinger L, Ballard D, Chen YF, Iversen P, Teicher BA. LY317615 decreases plasma VEGF levels in human tumor xenograft-bearing mice. Cancer Chemother Pharmacol 2004; 53: 133-140.

[15] Keepers YP, Pizao PE, Peters GJ, van Ark-Otte J, Winograd B, Pinedo HM. Comparison of the Sulforhodamine B Protein and Tetrazolium (MTT) assays for in vitro chemosensitivity testing. Eur J Cancer 1991; 27: 897-900.

[16] Chou TC and Talalay P. Quantitative analysis of dose-effect relationships: the combined effects of multiple drugs or enzyme inhibitors. Adv Enzyme Regul 1984; 22: 27-55.

[17] Bijnsdorp IV, Giovannetti E and Peters GJ. Analysis of drug interactions. Methods Mol Biol 2011; 731: 421-34.

[18] Avan A, Caretti V, Funel N, Galvani E, Maftouh M, Honeywell RJ, Lagerweij T, Van Tellingen O, Campani D, Fuchs D, Verheul HM, Schuurhuis GJ, Boggi U, Peters GJ, Würdinger T, Giovannetti E. Crizotinib inhibits metabolic inactivation of gemcitabine in c-Met-driven pancreatic carcinoma. Cancer Res 2013; 73: 6745-6756.

[19] Giovannetti E, Lemos C, Tekle C, Smid K, Nannizzi S, Rodriguez JA, Ricciardi S, Danesi R, Giaccone G, Peters GJ. Molecular mechanisms underlying the synergistic interaction of erlotinib, an epidermal growth factor receptor tyrosine kinase inhibitor, with the multitargeted antifolate pemetrexed in non-small-cell lung cancer cells. Mol Pharmacol 2008; 73: 1290-1300.

[20] Sigmond J, Backus HH, Wouters D, Temmink OH, Jansen G, Peters GJ. Induction of resistance to the multitargeted antifolate Pemetrexed (ALIMTA) in WiDr human colon cancer cells is associated with thymidylate synthase overexpression. Biochem Pharmacol 2003; 66: 431-438.

[21] Avan A, Adema AD, Hoebe EK, Huijts CM, Avan A, Veal GJ, Ruijtenbeek R, Wosikowski K, Peters GJ. Modulation of signaling enhances the efficacy of the combination of satraplatin and erlotinib. Curr Drug Targets 2014; 15: 1312-21.

[22] Shimokawa T, Seike M, Soeno C, Uesaka H, Miyanaga A, Mizutani H, Kitamura K, Minegishi Y, Noro R, Okano T, Yoshimura A, Gemma A. Enzastaurin has anti-tumour effects in lung cancers with overexpressed JAK pathway molecules. Br J Cancer 2012; 106: 867-75.

[23] Schwartz GK and Shah MA. Targeting the cell cycle: a new approach to cancer therapy. J Clin Oncol 2005; 23: 9408-9421.

[24] Black JD. Protein kinase C-mediated regulation of the cell cycle. Front Biosci 2000; 5: d406-423.

[25] Gu Y, Rosenblatt J and Morgan DO. Cell cycle regulation of CDK2 activity by phosphorylation of Thr160 and Tyr15. EMBO J 1992; 11: 3995-4005.

[26] Peng CY, Graves PR, Thoma RS, Wu Z, Shaw AS, Piwnica-Worms H. Mitotic and G2 checkpoint control: regulation of 14-3-3 protein binding by phosphorylation of Cdc25C on serine-216. Science 1997; 277: 1501-1505.

[27] Eckberg WR and Palazzo RE. Regulation of M-phase progression in chaetopterus oocytes by protein kinase C. Dev Biol 1992; 149: 395-405.

[28] Yu BZ, Zheng J, Yu AM, Shi XY, Liu Y, Wu DD, Fu W, Yang J. Effects of protein kinase C on M-phase promoting factor in early development of fertilized mouse eggs. Cell Biochem Funct 2004; 22: 291-298.
[29] Kawakami Y, Nishimoto H, Kitaura J, Maeda-Yamamoto M, Kato RM, Littman DR, Leitges M, Rawlings DJ, Kawakami T. Protein kinase C βII regulates Akt phosphorylation on Ser-473 in a cell type- and stimulus-specific fashion. J Biol Chem 2004; 279: 47720-47725.
[30] Burgering BM and Coffer PJ. Protein kinase B (c-Akt) in phosphatidylinositol-3-OH kinase signal transduction. Nature 1995; 376: 599-602.
[31] Jorissen RN, Walker F, Pouliot N, Garrett TP, Ward CW, Burgess AW. Epidermal growth factor receptor: mechanisms of activation and signalling. Exp Cell Res 2003; 284: 31-53.
[32] Zhang J, Anastasiadis PZ, Liu Y, Thompson EA, Fields AP. Protein kinase C (PKC) βII induces cell invasion through a Ras/Mek-, PKC iota/Rac 1-dependent signaling pathway. J Biol Chem 2004; 279: 22118-23.
[33] Goode N, Hughes K, Woodgett JR, Parker PJ. Differential regulation of glycogen synthase kinase-3β by protein kinase C isotypes. J Biol Chem 1992; 267: 16878-16882.
[34] Rizvi MA, Ghias K, Davies KM, Ma C, Weinberg F, Munshi HG, Krett NL, Rosen ST, J54 Enzastaurin (LY317615), a protein kinase Cβ inhibitor, inhibits the AKT pathway and induces apoptosis in multiple myeloma cell lines. Mol Cancer Ther 2006; 5: 1783-9.
[35] Herbst RS, Oh Y, Wagle A, Lahn M. Enzastaurin, a protein kinase Cβ- selective inhibitor, and its potential application as an anticancer agent in lung cancer. Clin Cancer Res 2007; 13: s4641-6.
[36] Oh Y, Herbst RS, Burris H, Cleverly A, Musib L, Lahn M, Bepler G. Enzastaurin, an oral serine/threonine kinase inhibitor, as second- or third-line therapy of non-small-cell lung cancer. J Clin Oncol 2008; 26: 1135-1141.
[37] Giovannetti E, Honeywell R, Hanauske AR, Tekle C, Kuenen B, Sigmond J, Giaccone G, Peters GJ. Pharmacological aspects of the enzastaurin-pemetrexed combination in non-small cell lung cancer (NSCLC). Curr Drug Targets 2010; 11: 12-28.
[38] Zhang G, Fang B, Liu RZ, Lin H, Kinose F, Bai Y, Oguz U, Remily-Wood ER, Li J, Altiok S, Eschrich S, Koomen J, Haura EB. Mass spectrometry mapping of epidermal growth factor receptor phosphorylation related to oncogenic mutations and tyrosine kinase inhibitor sensitivity. J Proteome Res 2011; 10: 305-319.
[39] Saito Y, Vandenheede JR, and Cohen P. The mechanism by which epidermal growth factor inhibits glycogen synthase kinase 3 in A431 cells. Biochem J 1994; 303: 27-31.
[40] Gao C, Chen G, Kuan SF, Zhang DH, Schlaepfer DD, Hu J. FAK/PYK2 promotes the Wnt/β-catenin pathway and intestinal tumorigenesis by phosphorylating GSK3β. Elife 2015;4:1-17.
[41] MacDonald B, Tamai K and He X. Wnt/β-catenin signaling: components, mechanisms, and diseases. Dev Cell 2009; 17: 9-26.
[42] Pasquale EB. Eph receptors and ephrins in cancer: bidirectional signalling and beyond. Nat Rev Cancer 2010; 10: 165-180.
[43] Wang J, Dong Y, Wang X, Ma H, Sheng Z, Li G, Lu G, Sugimura H, Zhou X. Expression of EphA1 in gastric carcinomas is associated with metastasis and survival. Oncol Rep 2010; 24: 1577-1584.
[44] Chen G, Wang Y, Zhou M, Shi H, Yu Z, Zhu Y, Yu F. EphA1 receptor silencing by small interfering RNA has antiangiogenic and antitumor efficacy in hepatocellular carcinoma. Oncol Rep 2010; 23: 563-570.
[45] Giaginis C, Tsoukalas N, Bournakis E, Alexandrou P, Kavantzas N, Patsouris E, Theocharis S. Ephrin (Eph) receptor A1, A4, A5 and A7 expression in human non-small cell lung carcinoma: associations with clinicopathological parameters, tumor proliferative capacity and patients' survival. BMC Clin Pathol 2014; 14: 8.
[46] Peng L, Wang H, Dong Y, Ma J, Wen J, Wu J, Wang X, Zhou X, Wang J. Increased expression of EphA1 protein in prostate cancers correlates with high Gleason score. Int J Clin Exp Pathol 2013; 6: 1854-1860.
[47] Wang J, Ma J, Dong Y, Shen Z, Ma H, Wang X, Shi S, Wu J, Lu G, Peng L, Zhoud X. High expression of EphA1 in esophageal squamous cell carcinoma is associated with lymph node metastasis and advanced disease. APMIS 2013; 121: 30-7.
[48] Yamazaki T, Masuda J, Omori T, Usui R, Akiyama H, Maru Y. EphA1 interacts with integrin-linked kinase and regulates cell morphology and motility. J Cell Sci 2009; 122: 243-255.
[49] Boyd AW, Lackmann M. Signals from Eph and ephrin proteins: a developmental tool kit. Sci STKE 2001; 2001: re20.
[50] Zarubin T and Han J. Activation and signaling of the p38 MAP kinase pathway. Cell Res 2005; 15: 11-18.
[51] Guo K, Liu Y, Zhou H, Dai Z, Zhang J, Sun R, Chen J, Sun Q, Lu W, Kang X, Chen P. Involvement of protein kinase C β-extracellular signal-regulating kinase 1/2/p38 mitogen-activated protein kinase-heat shock protein 27 activation in hepatocellular carcinoma cell motility and invasion. Cancer Sci 2008; 99: 486-96.
[52] Park SH, Seong MA, Lee HY. p38 MAPK-induced MDM2 degradation confers paclitaxel resistance through p53-mediated regulation of

EGFR in human lung cancer cells. Oncotarget 2016; 7: 8184-8199.
[53] Nishimura Y, Bereczky B, Ono M. The EGFR inhibitor gefitinib suppresses ligand-stimulated endocytosis of EGFR via the early/late endocytic pathway in non-small cell lung cancer cell lines. Histochem Cell Biol 2007; 127: 541-553.
[54] Gelardi T, Caputo R, Damiano V, Daniele G, Pepe S, Ciardiello F, Lahn M, Bianco R, Tortora G. Enzastaurin inhibits tumours sensitive and resistant to anti-EGFR drugs. Br J Cancer 2008; 99: 473-480.
[55] Wick W, Steinbach JP, Platten M, Hartmann C, Wenz F, von Deimling A, Shei P, Moreau-Donnet V, Stoffregen C, Combs SE. Enzastaurin before and concomitant with radiation therapy, followed by enzastaurin maintenance therapy, in patients with newly diagnosed glioblastoma without MGMT promoter hypermethylation. Neuro Oncol 2013; 15: 1405-1412.
[56] Ouaret D and Larsen AK. Protein kinase Cβ inhibition by enzastaurin leads to mitotic missegregation and preferential cytotoxicity toward colorectal cancer cells with chromosomal instability (CIN). Cell Cycle 2014; 13: 2697-2706.
[57] Mochly-Rosen D, Das K, Grimes KV. Protein kinase C, an elusive therapeutic target?. Nat Rev Drug Discov 2012; 11: 937-957.